Journal of Sound and Vibration (1997) **201**(2), 235–253

THE RESPONSE OF TWO-DIMENSIONAL PERIODIC STRUCTURES TO IMPULSIVE POINT LOADING

R. S. LANGLEY

Department of Aeronautics and Astronautics, University of Southampton, Southampton SO17 1BJ, England

(*Received* 13 *May* 1996, *and in final form* 6 *September* 1996)

This work is concerned with the response of an infinite two-dimensional periodic structure to an impulsive point load or, equivalently, the response of a finite system at times before the disturbance reaches the system boundaries. Initially, a modal approach is employed to yield an expression for the response of a finite system under Born–von Kármán boundary conditions. By allowing the system size to become large, the modal response summation is converted to an integral and the method of stationary phase is employed, with due allowance being made for the occurrence of caustics. With this approach, the response is expressed in terms of the properties of the "phase constant surfaces" which arise in the analysis of plane wave motion through the system. The method is applied to an example lumped mass system and a comparison is made with results yielded by direct numerical simulation. The method is found to be efficient and accurate, and a number of observations are made regarding the physical nature of the system response.

1. INTRODUCTION

A two-dimensional periodic structure consists of a number of identical units which are connected together in a regular pattern to form a repetitive structural geometry—as an example, an orthogonally stiffened plate can be considered to be a two-dimensional periodic structure in which the basic unit is an edge stiffened panel. The widespread occurrence of periodic or near-periodic structures in engineering has lead to much research regarding the dynamic behaviour of such structures, and the latest developments in this area have been summarized in two recent review papers [1, 2]. Attention has tended to be focused on the nature of free elastic wave motion through the structure [3, 4] or on the response of the structure to pressure wave excitation [5]. The fact that periodic structures can be subjected to localized excitation sources, arising for example from equipment mounts, has led to a recent study concerning the response of a two-dimensional periodic structure to harmonic point loading [6]. It was found that the structural response can at some frequencies exhibit a very distinctive spatial pattern associated with the occurrence of caustics, and in particular that "dead zones" of almost zero response can occur. The aim of the present work is to extend this analysis to the case of an impulsive point load, in order to investigate the extent to which the nature of the behaviour under harmonic loading is also evidenced under shock loading.

The present analysis is concerned with the impulse response of an infinite system, or equivalently the impulse response of a finite system at times before the disturbance reaches the system boundaries. As in reference [6], the analysis is based on considering initially the

0022–460X/97/120235 + 19 $25.00/0/sv960744

response of a finite system under periodic or Born–von Kármán boundary conditions. This leads to a relatively straight forward expression for the impulse response of the system in the form of a modal summation. By allowing the system size to become large, this summation is converted into an integral, and the method of stationary phase is then applied to yield an analytical result for the response of an infinite system. This result is not valid in the vicinity of a caustic (that is, a time at which there is a change in the number of stationary points associated with the method of stationary phase) and the analysis is modified accordingly to cater for this difficulty. The method is applied to an example system consisting of a two-dimensional array of lumped masses, and a comparison is made with a direct numerical simulation of the system response. It is found that the method of stationary phase yields an efficient and accurate solution which helps to reveal physical aspects of the system response. The spatial distribution of the maximum response is found to be of a distinctive pattern which is closely related to previous results regarding the case of harmonic loading [6].

2. THE IMPULSE RESPONSE OF A TWO-DIMENSIONAL PERIODIC STRUCTURE

2.1. MODAL FORMULATION AND EXTENSION TO THE INFINITE SYSTEM

A two-dimensional periodic structure consists of a basic unit which is repeated in two directions to form a regular pattern, as shown schematically in Figure 1. Each unit shown in this figure might represent, for example, an edge stiffened curved panel in an aircraft fuselage structure, a three-dimensional beam assembly in a roof truss structure, or a pair of strings in the form of a "+" in a cable net structure. The displacement $\mathbf{w}$ of the system at some time t can be written in the form $\mathbf{w}(\mathbf{n}, \mathbf{x}, t)$, where $\mathbf{n} = (n_1\ n_2)$ identifies a particular unit and $\mathbf{x} = (x_1\ x_2\ x_3)$ identifies a particular point within the unit. The co-ordinate system $\mathbf{x}$ is taken to be local to each unit, and the precise dimension of both $\mathbf{x}$ and the response vector $\mathbf{w}$ will depend on the details of the system under consideration.

The present work is concerned with the response of a two-dimensional periodic structure to impulsive point loading. In the case of an undamped system of finite dimension, the

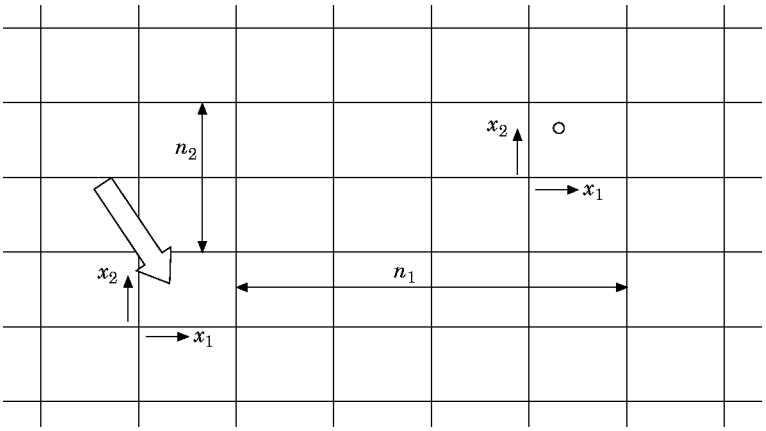

Figure 1. A schematic of a two-dimensional periodic structure. The arrow indicates the reference unit (with $\mathbf{n} = \mathbf{0}$), while the circle represents a general point $(\mathbf{n}, \mathbf{x})$. The structure may have a third spatial co-ordinate x_3, which is not shown in the present schematic.

response at location $(\mathbf{n}, \mathbf{x})$ to an impulsive force $\mathbf{F}$ applied at $(\mathbf{0}, \mathbf{x}_0)$ can be expressed in the standard form [7]

$$\mathbf{w}(\mathbf{n}, \mathbf{x}, t) = \sum_p \sum_q \boldsymbol{\phi}_{pq}(\mathbf{n}, \mathbf{x})\mathbf{F}^{\mathrm{T}}\boldsymbol{\phi}_{pq}(\mathbf{0}, \mathbf{x}_0)(1/\omega_{pq}) \sin \omega_{pq} t, \tag{1}$$

where $\boldsymbol{\phi}_{pq}(\mathbf{n}, \mathbf{x})$ are the modes of vibration of the system and ω_{pq} are the associated natural frequencies; the modes $\boldsymbol{\phi}_{pq}$ which appear in equation (1) are scaled to unit generalized mass, so that

$$\sum_{n_1} \sum_{n_2} \int_V \rho(\mathbf{x})\boldsymbol{\phi}_{pq}^{\mathrm{T}}(\mathbf{n}, \mathbf{x})\boldsymbol{\phi}_{pq}(\mathbf{n}, \mathbf{x})\, \mathrm{d}\mathbf{x} = 1, \tag{2}$$

where V represents the volume (or equivalent) of a unit and $\rho(\mathbf{x})$ is the mass density. The present concern is with the impulse response of an infinite system or, equivalently, the impulse response of a finite system at times before the disturbance reaches the system boundaries. In this case, the response is independent of the system boundary conditions, and it follows that any analytically convenient set of modes can be employed in equation (1). As explained in reference [6], it is expedient to consider the Born–Von Kármán (or "periodic") boundary conditions, as in this case the modes of vibration can be expressed very simply in terms of propagating plane wave components. In this regard it can be noted from periodic structure theory [8, 9] that a propagating plane wave of frequency ω has the general form

$$\mathbf{w}(\mathbf{n}, \mathbf{x}, t) = \mathrm{Re}\{\mathbf{g}(\mathbf{x}) \exp(\mathrm{i}\varepsilon_1 n_1 + \mathrm{i}\varepsilon_2 n_2 + \mathrm{i}\omega t)\}, \tag{3}$$

where ε_1 and ε_2 are known as the propagation constants of the wave (with $-\pi < \varepsilon_1 \leqslant \pi$ and $-\pi < \varepsilon_2 \leqslant \pi$ for uniqueness), and $\mathbf{g}(\mathbf{x})$ is a complex amplitude function. By considering the dynamics of a single unit of the system and applying Bloch's theorem [8], it is possible to derive a dispersion equation which must be satisfied by the triad $(\omega, \varepsilon_1, \varepsilon_2)$—by specifying ε_1 and ε_2 this equation can be solved to yield the admissible propagation frequencies ω. By way of an example, the solutions yielded by this procedure for a plate which rests on a grillage of simple supports are shown in Figure 2 (after reference [3]). It is clear that the solutions form surfaces above the ε_1–ε_2 plane—these surfaces are usually referred to as "phase constant" surfaces, and a single surface will be represented here by the equation $\omega = \Omega(\varepsilon_1, \varepsilon_2)$. The phase constant surfaces always have cyclic symmetry of order two, so that $\Omega(\varepsilon_1, \varepsilon_2) = \Omega(-\varepsilon_1, -\varepsilon_2)$; for an orthotropic system the surfaces also have cyclic symmetry of order four, and therefore only the first quadrant of the ε_1–ε_2 plane need be considered explicitly, as in Figure 2.

The key point about the Born–Von Kármán boundary conditions is that a single propagating wave can fully satisfy these conditions provided that ε_1 and ε_2 are chosen appropriately. The conditions state that the left-hand edge of the system is contiguous with the right-hand edge, and similarly that the top edge is contiguous with the bottom edge, so that the system behaves as if it were topologically equivalent to a torus. If the system is comprised of $N_1 \times N_2$ units, then a propagating wave will satisfy these conditions if $\varepsilon_1 N_1 = 2\pi p$ and $\varepsilon_2 N_2 = 2\pi q$, for any integers p and q. Following equation (3), the displacement associated with such a wave can be written in the form

$$\mathbf{w}_{pq}(\mathbf{n}, \mathbf{x}, t) = \mathrm{Re}\,\{\mathbf{g}_{pq}(\mathbf{x}) \exp(\mathrm{i}\varepsilon_{1p} n_1 + \mathrm{i}\varepsilon_{2q} n_2 + \mathrm{i}\omega_{pq} t)\}, \tag{4}$$

where ε_{1p} and ε_{2q} are the appropriate values of the phase constants, and $\omega_{pq} = \Omega(\varepsilon_{1p}, \varepsilon_{2q})$. Now since $\Omega(\varepsilon_{1p}, \varepsilon_{2q}) = \Omega(-\varepsilon_{1p}, -\varepsilon_{2q})$, it follows that a wave of frequency ω_{pq} travelling

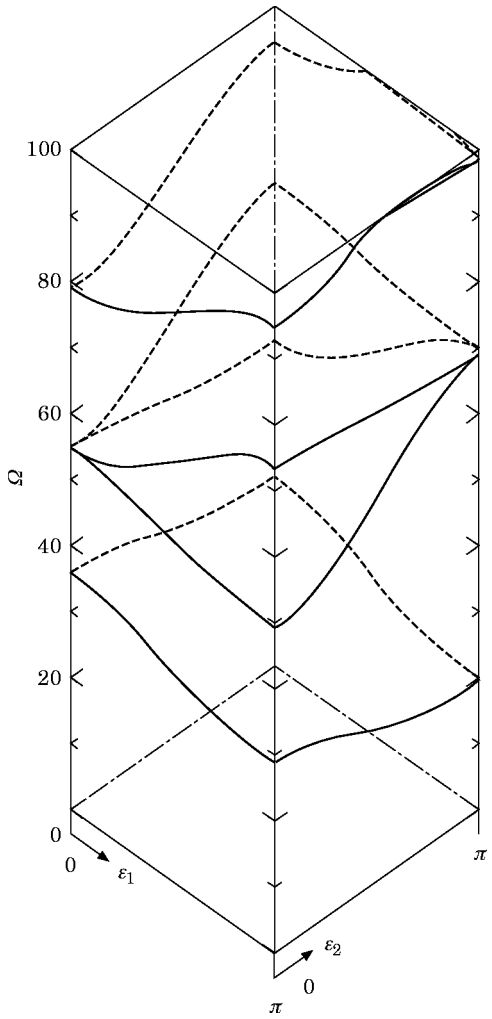

Figure 2. Phase constant surfaces for a plate which rests on a square grillage of simple supports. Ω is a non-dimensional frequency, defined as $\Omega = \omega L^2\sqrt{(m/D)}$, where m and D are, respectively, the mass per unit area and the flexural rigidity of the plane, and L is the support spacing.

in the opposite direction to $\mathbf{w}_{pq}$ will also satisfy the boundary conditions. This wave ($\mathbf{w}'_{pq}$, say) will have the form

$$\mathbf{w}'_{pq}(\mathbf{n}, \mathbf{x}, t) = \mathrm{Re}\,\{\mathbf{g}^*_{pq}(\mathbf{x})\exp(-\mathrm{i}\varepsilon_{1p}n_1 - \mathrm{i}\varepsilon_{2q}n_2 + \mathrm{i}\omega_{pq}t)\}, \tag{5}$$

where it has been noted from periodic structure theory that reversing the direction of a wave leads to the conjugate of the complex amplitude function $\mathbf{g}(\mathbf{x})$. The two waves represented by equations (4) and (5) can be combined with the appropriate phase to produce two modes of vibration of the system in the form

$$\begin{Bmatrix}\boldsymbol{\phi}_{1pq}(\mathbf{n}, \mathbf{x})\\ \boldsymbol{\phi}_{2pq}(\mathbf{n}, \mathbf{x})\end{Bmatrix} = \begin{Bmatrix}\mathrm{Re}\\ \mathrm{Im}\end{Bmatrix}\mathbf{g}_{pq}(\mathbf{x})\exp(\mathrm{i}\varepsilon_{1p}n_1 + \mathrm{i}\varepsilon_{2q}n_2). \tag{6}$$

By adopting this set of modes, it can be shown [6] that equation (1) can be re-expressed as

$$\mathbf{w}(\mathbf{n}, \mathbf{x}, t) = \sum_{p=1-N_1/2}^{N_1/2} \sum_{q=1-N_2/2}^{N_2/2} 2\mathbf{g}_{pq}^*(\mathbf{x})\mathbf{F}^{\mathrm{T}}\mathbf{g}_{pq}(\mathbf{x}_0) \exp(-\mathrm{i}\varepsilon_{1p}n_1 - \mathrm{i}\varepsilon_{2q}n_2)(1/\omega_{pq}) \sin \omega_{pq} t, \quad (7)$$

where N_1 and N_2 have been taken to be even, and the amplitude function $\mathbf{g}_{pq}$ is scaled so that

$$\mathbf{g}_{pq} = [2\rho(\mathbf{x})VN_1N_2]^{-1/2}\mathbf{f}_{pq}(\mathbf{x}), \qquad (1/V)\int_V \mathbf{f}_{pq}^{\mathrm{T}}(\mathbf{x})\mathbf{f}_{pq}^*(\mathbf{x})\,\mathrm{d}\mathbf{x} = 1, \quad (8, 9)$$

where the normalized amplitude function $\mathbf{f}_{pq}$ is defined accordingly. The summation which appears in equation (7) includes only those modes associated with a single phase constant surface $\Omega(\varepsilon_1, \varepsilon_2)$; if more than one surface occurs, then the equation should be summed over the complete set of surfaces. The summation will include N_1N_2 modes for each surface, which is consistent with known results for the modal density of a two-dimensional periodic structure.

Equation (7) yields the response of a finite system of dimension $N_1 \times N_2$ to an impulsive point load—this response is identical to that of an infinite system at times before the disturbance reaches the system boundaries. If the system size is allowed to tend to infinity in equation (7), then neighbouring values of the phase constants ε_{1p} and ε_{2q} become closely spaced (since $\mathrm{d}\varepsilon_{1p} = \varepsilon_{1,p+1} - \varepsilon_{1p} = 2\pi/N_1$ and $\mathrm{d}\varepsilon_{2q} = \varepsilon_{2,q+1} - \varepsilon_{2q} = 2\pi/N_2$), and in this case the summations can be replaced by integrals over the phase constants, to yield

$$\mathbf{w}(\mathbf{n}, \mathbf{x}, t) = (N_1N_2/2\pi^2)\int_{-\pi}^{\pi}\int_{-\pi}^{\pi} \mathbf{g}^*(\mathbf{x})\mathbf{F}^{\mathrm{T}}\mathbf{g}(\mathbf{x}_0) \exp(-\mathrm{i}\varepsilon_1 n_1 - \mathrm{i}\varepsilon_2 n_2)(1/\omega) \sin \omega t\, \mathrm{d}\varepsilon_1\, \mathrm{d}\varepsilon_2, \quad (10)$$

where $\omega = \Omega(\varepsilon_1, \varepsilon_2)$ and $\mathbf{g}(\mathbf{x})$ is the complex amplitude associated with the wave $(\omega, \varepsilon_1, \varepsilon_2)$. Equation (10) can also be written in the form

$$\mathbf{w}(\mathbf{n}, \mathbf{x}, t) = (1/4V\pi^2)[\rho(\mathbf{x})\rho(\mathbf{x}_0)]^{-1/2}\int_{-\pi}^{\pi}\int_{-\pi}^{\pi} \mathbf{f}^*(\mathbf{x})\mathbf{F}^{\mathrm{T}}\mathbf{f}(\mathbf{x}_0) \times \exp(-\mathrm{i}\varepsilon_1 n_1 - \mathrm{i}\varepsilon_2 n_2)(1/\omega) \sin \omega t\, \mathrm{d}\varepsilon_1\, \mathrm{d}\varepsilon_2, \quad (11)$$

which highlights the fact that the response is independent of N_1 and N_2, as should be the case for an infinite system. Equation (10) or (11) can be evaluated by numerical integration for fixed values of $\mathbf{n}$, $\mathbf{x}$ and t. If the trapezoidal rule is employed, then the equation essentially reduces to equation (7), with N_1 and N_2 in this case representing the number of intervals which are employed in the numerical method. It is clear that more intervals are needed as the time t increases, since $N_1/2$ and $N_2/2$ must always exceed the distance travelled by the disturbance if (real or numerical) reflections from the system boundaries are to be avoided. Clearly, the numerical evaluation of equation (11) can be computationally demanding, and thus an approximate analytical approach which is based on the method of stationary phase [10] is presented in the following sections.

2.2. APPLICATION OF THE METHOD OF STATIONARY PHASE

In order to apply the method of stationary phase to equation (11) it is useful to rewrite the equation in the form

$$\mathbf{w}(\mathbf{n}, \mathbf{x}, t) = (1/4V\pi^2)[\rho(\mathbf{x})\rho(\mathbf{x}_0)]^{-1/2}\,\mathrm{Re}\left\{-\mathrm{i}\int_{-\pi}^{\pi}\int_{-\pi}^{\pi}(1/\Omega)\mathbf{f}^*(\mathbf{x})\mathbf{F}^{\mathrm{T}}\mathbf{f}(\mathbf{x}_0)\right.$$

$$\left.\times\exp(-\mathrm{i}\varepsilon_1 n_1 - \mathrm{i}\varepsilon_2 n_2 + \mathrm{i}\Omega t)\,\mathrm{d}\varepsilon_1\,\mathrm{d}\varepsilon_2\right\}, \quad (12)$$

where use has been made of the properties of Ω and $\mathbf{f}$ with regard to a sign reversal in ε_1 and ε_2 (that is, Ω is unchanged whereas $\mathbf{f}$ is replaced by $\mathbf{f}^*$). The method of stationary phase is based on the premise that the major contribution to the integral which appears in equation (12) arises from those regions of the ε_1–ε_2 plane which are in the immediate vicinity of points at which the phase $-\varepsilon_1 n_1 - \varepsilon_2 + \Omega t$ is stationary with respect to both ε_1 and ε_2 [10]. The conditions for a stationary point are

$$n_1 = (\partial\Omega/\partial\varepsilon_1)t, \qquad n_2 = (\partial\Omega/\partial\varepsilon_2)t. \quad (13, 14)$$

These conditions have a clear physical interpretation, since the group velocity of wave motion in a two-dimensional periodic structure (in units of bays per second) is given by $c_{g1} = \partial\Omega/\partial\varepsilon_1$ in the x_1 direction and $c_{g2} = \partial\Omega/\partial\varepsilon_2$ in the x_2 direction [11]: the values of ε_1 and ε_2 yielded by equations (13) and (14) are therefore associated with a wave which travels from the excited bay to bay $\mathbf{n}$ in time t. The method of stationary phase proceeds by expanding Ω about a stationary point, $(\varepsilon_{1s}\ \varepsilon_{2s})$ say, to yield

$$-\varepsilon_1 n_1 - \varepsilon_2 n_2 + \Omega t \approx -\varepsilon_{1s} n_1 - \varepsilon_{2s} n_2 + \Omega_s t + (t/2)\{(\partial^2\Omega/\partial\varepsilon_1^2)(\varepsilon_1 - \varepsilon_{1s})^2$$

$$+ 2(\partial^2\Omega/\partial\varepsilon_1\,\partial\varepsilon_2)(\varepsilon_1 - \varepsilon_{1s})(\varepsilon_2 - \varepsilon_{2s}) + (\partial^2\Omega/\partial\varepsilon_2^2)(\varepsilon_2 - \varepsilon_{2s})^2\}, \quad (15)$$

where $\Omega_s \equiv \Omega(\varepsilon_{1s}, \varepsilon_{2s})$ and all the derivatives of Ω are evaluated at the stationary point. If equation (15) is substituted into equation (12), then the double integral can be evaluated by assuming that (i) all terms which appear in the integrand are constant (and evaluated at the stationary point) other than those which depend explicitly on ε_1 and ε_2 in equation (15), and (ii) the integration range can be extended from $(-\pi\ \pi)$ to $(-\infty\ \infty)$, since the contribution from regions which are remote from the stationary point is negligible. The integral is then of the standard Gaussian type, and can be evaluated to yield [10]

$$\mathbf{w}(\mathbf{n}, \mathbf{x}, t) = (1/2V\pi)[\rho(\mathbf{x})\rho(\mathbf{x}_0)|J|]^{-1/2}\,\mathrm{Re}\{-(\mathrm{i}/\Omega t)\mathbf{f}^*(\mathbf{x})\mathbf{F}^{\mathrm{T}}\mathbf{f}(\mathbf{x}_0)$$

$$\times\exp(-\mathrm{i}\varepsilon_1 n_1 - \mathrm{i}\varepsilon_2 n_2 + \mathrm{i}\Omega t + \mathrm{i}\delta)\}, \quad (16)$$

where all terms are evaluated at the stationary point (the suffix s is omitted for ease of notation), and J and δ are defined as

$$J = (\partial^2\Omega/\partial\varepsilon_1^2)(\partial^2\Omega/\partial\varepsilon_2^2) - (\partial^2\Omega/\partial\varepsilon_1\,\partial\varepsilon_2)^2, \quad (17)$$

$$\delta = (\pi/4)\,\mathrm{sgn}\,(\partial^2\Omega/\partial\varepsilon_1^2)\{1 + \mathrm{sgn}\,(J)\}. \quad (18)$$

In practice, there may be multiple stationary points at which equations (13) and (14) are satisfied: in this case, equation (16) should be summed over all such points.

Equation (16) will clearly yield a poor approximation to the response if $J \approx 0$. Generally, J will be close to zero in the vicinity of a *caustic* [10]: that is, a time at which the number of stationary points yielded by equations (13) and (14) either increases or decreases. The situation in which the number of stationary points increases at $t = t_0$ is addressed in what follows, and the two cases $t > t_0$ and $t < t_0$ (with $t \approx t_0$) are considered in detail in the following sections. For $t > t_0$ it is sufficient to include a number of higher order terms in the expansion represented by equation (15); for $t < t_0$ it is necessary to consider a contribution from the additional stationary point associated with $t = t_0$—although this is not strictly

a stationary point for $t < t_0$, the values of the integrand in the vicinity of this point can make a significant contribution to equation (12) for $t \approx t_0$. It can be noted that the analysis contained in the following sections should be interchanged for the contrary case in which the number of stationary points decreases at $t = t_0$.

2.2.1. *Detailed analysis of the case* $t \approx t_0$ $(J \approx 0)$ *with* $t > t_0$

In this case the approximation afforded by equation (15) can be improved by including a number of higher order terms in the Taylor series expansion of Ω. To this end it is helpful to rotate the $(\varepsilon_1\ \varepsilon_2)$ co-ordinate system to a new system $(p_1\ p_2)$, which is chosen to make $\partial^2\Omega/\partial p_1\,\partial p_2 = 0$ at the stationary point. This can be achieved by putting $p_1 = \varepsilon_1 \cos\theta + \varepsilon_2 \sin\theta$ and $p_2 = -\varepsilon_1 \sin\theta + \varepsilon_2 \cos\theta$, where

$$\tan 2\theta = 2(\partial^2\Omega/\partial\varepsilon_1\,\partial\varepsilon_2)/(\partial^2\Omega/\partial\varepsilon_1^2 - \partial^2\Omega/\partial\varepsilon_2^2). \tag{19}$$

Equation (19) yields two solutions for θ in the form $\{\theta, \theta + \pi/2\}$, and it is convenient to adopt that solution for which $\partial^2\Omega/\partial p_1^2 = 0$ at $t = t_0$ (it should be noted that since $J = 0$ at $t = t_0$, and by definition $\partial^2\Omega/\partial p_1\,\partial p_2 = 0$, it follows that either $\partial^2\Omega/\partial p_1^2 = 0$ or $\partial^2\Omega/\partial p_2^2 = 0$ at t_0). Equation (15) can now be replaced by

$$-\varepsilon_1 n_1 - \varepsilon_2 n_2 + \Omega t \approx -\varepsilon_{1s} n_1 - \varepsilon_{2s} n_2 + \Omega_s t + (t/2)\{(\partial^2\Omega/\partial p_1^2)(p_1 - p_{1s})^2 + (1/3)(\partial^3\Omega/\partial p_1^3)(p_1 - p_{1s})^3 + (\partial^2\Omega/\partial p_2^2)(p_2 - p_{2s})^2\}, \tag{20}$$

where third order terms involving p_2 are omitted, since $\partial^2\Omega/\partial p_2^2$ does not approach zero in the vicinity of t_0. If equation (20) is substituted into equation (12), and the integration variables are changed from $(\varepsilon_1\ \varepsilon_2)$ to $(p_1\ p_2)$, then the double integral can be evaluated as (i) a Gaussian type integral over p_2, and (ii) an Airy type integral over p_1. This procedure yields [6, 10]

$$\mathbf{w}(\mathbf{n}, \mathbf{x}, t) = (1/4V\pi^2)[\rho(\mathbf{x})\rho(\mathbf{x}_0)]^{-1/2}\,\mathrm{Re}\{-(\mathrm{i}/\Omega)\mathbf{f}^*(\mathbf{x})\mathbf{F}^{\mathrm{T}}\mathbf{f}(\mathbf{x}_0) \times \exp(-\mathrm{i}\varepsilon_1 n_1 - \mathrm{i}\varepsilon_2 n_2 + \mathrm{i}\Omega t)AG\}, \tag{21}$$

where G is the result of the Gaussian integral, so that

$$G = (2\pi)^{1/2}(t\partial^2\Omega/\partial p_2^2)^{-1/2} \exp[\mathrm{i}(\pi/4)\,\mathrm{sgn}(\partial^2\Omega/\partial p_2^2)], \tag{22}$$

and A is the result of the Airy type integral, so that [6, 10]

$$A = \pi|3a_3|^{-1/3} \exp(-2\mathrm{i}a_2^3/27a_3^2)\{\mathrm{Ai}(-z) - \mathrm{i}\,\mathrm{sgn}\,(a_2)\,\mathrm{Bi}\,(-z)\}, \tag{23}$$

where

$$a_2 = -(t/2)\partial^2\Omega/\partial p_1^2, \quad a_3 = -(t/6)\partial^3\Omega/\partial p_1^3, \quad z = |3a_3|^{-1/3}|a_2^2/3a_3|. \tag{24a–26}$$

It can be confirmed that equation (21) reduces to equation (16) if the third order term $\partial^3\Omega/\partial p_1^3$ is neglected; for $J \approx 0$ this term has a strong influence on the response $\mathbf{w}$, as will be shown in section 3 for a particular numerical example. In summary, the total response at time $t > t_0$ is given by the summation of equation (16) over each stationary point, although for stationary points with $J \approx 0$ equation (16) must be replaced by equation (21).

2.2.2. *Detailed analysis of the case* $t \approx t_0$ $(J \approx 0)$ *with* $t < t_0$

It has been supposed that a greater number of stationary points occur for $t > t_0$ than for $t < t_0$, so that the time t_0 represents a caustic. Typically, as will be shown for a particular example in section 3, *two* additional stationary points will occur for $t > t_0$: as t is reduced towards t_0, these stationary points approach each other, and ultimately they become a single stationary point, $(\varepsilon_{10}\ \varepsilon_{20})$ say, at $t = t_0$. For $t < t_0$, the occurrence of the stationary

point at t_0 can strongly influence the integral which appears in equation (12), even though this stationary point does not satisfy the stationary conditions, equations (13) and (14), at times other than t_0. An allowance for this effect can be made by expanding the phase $-\varepsilon_1 n_1 - \varepsilon_2 n_2 + \Omega t$ about $(\varepsilon_{10}\, \varepsilon_{20})$, to yield

$$-\varepsilon_1 n_1 - \varepsilon_2 n_2 + \Omega t = -\varepsilon_{10} n_1 - \varepsilon_{20} n_2 + \Omega_0 t - (n_1 \cos\theta + n_2 \sin\theta)(p_1 - p_{10}) + (t/2)\{2(\partial\Omega/\partial p_1)(p_1 - p_{10}) + (1/3)(\partial^3\Omega/\partial p_1^3)(p_1 - p_{10})^3 + (\partial^2\Omega/\partial p_2^2)(p_2 - p_{20})^2\}, \quad (27)$$

where all of the partial derivatives are evaluated at the point $(\varepsilon_{10}\, \varepsilon_{20})$, and the co-ordinates p_1, p_2 and θ are as defined in the previous section, so that $\partial^2\Omega/\partial p_1\, \partial p_2 = \partial^2\Omega/\partial p_1^2 = 0$ at $t = t_0$. It can be noted that first and third order terms in $(p_2 - p_{20})$ are omitted from equation (27) on the assumption that the second order term will dominate for $t \approx t_0$, as it certainly does for $t = t_0$. If equation (27) is substituted into equation (12), then the contribution to **w** arising from the vicinity of $(\varepsilon_{10}\, \varepsilon_{20})$ in the ε_1–ε_2 plane can be evaluated as a Gaussian integral over p_2 and as an Airy type integral over p_1. This again leads to equation (21), with G given by equation (22), although in this case equation (23) is replaced by the result [6]

$$A = 2\pi|(t/2)(\partial^3\Omega/\partial p_1^3)|^{-1/3}\, \mathrm{Ai}\,(z), \quad (28)$$

$$z = |(t/2)(\partial^3\Omega/\partial p_1^3)|^{-1/3}|n_1 \cos\theta + n_2 \sin\theta - t(\partial\Omega/\partial p_1)|. \quad (29)$$

The total response at the time $t < t_0$ will then consist of (i) a contribution in the form of equation (16) arising from each stationary point, and (ii) a contribution in the form of equation (21) (with G and A given by equations (22) and (28) respectively) which accounts for the effect of the caustic at t_0.

3. NUMERICAL EXAMPLE

3.1. THE SYSTEM CONSIDERED

An example of a two-dimensional periodic structure is shown schematically in Figure 3: the structure consists of a rectangular grid of lumped masses m which are coupled through

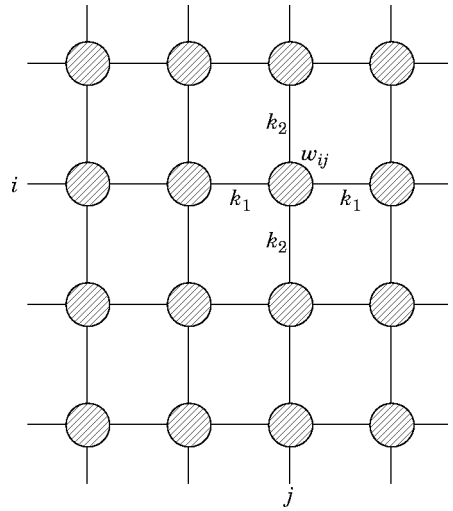

Figure 3. A schematic of a two-dimensional mass–spring periodic system. Each mass has a single out-of-plane degree of freedom and is attached to earth by a spring of stiffness k.

horizontal and vertical shear springs of stiffness k_1 and k_2 respectively. Each mass has a single degree of freedom consisting of the out-of-plane displacement w, and a linear spring of stiffness k is attached between each mass and a fixed base. By letting w_{ij} represent the displacement of the ijth mass, where i and j are shown in Figure 3, the equations of motion of the system can be written in the form

$$m\ddot{w}_{ij} + (k + 2k_1 + 2k_2)w_{ij} - k_1(w_{i,j-1} + w_{i,j+1}) - k_2(w_{i-1,j} + w_{i+1,j}) = 0. \tag{30}$$

The dispersion relation for harmonic plane wave motion of frequency ω can be derived by employing Bloch's theorem [8] which, in the present context, states that

$$w_{ij} = e^{i\varepsilon_1} w_{i,j-1} = e^{-i\varepsilon_1} w_{i,j+1} = e^{i\varepsilon_2} w_{i-1,j} = e^{-i\varepsilon_2} w_{i+1,j}, \tag{31}$$

where ε_1 and ε_2 are the propagation constants. Equations (30) and (31) yield the result

$$\Omega^2(\varepsilon_1, \varepsilon_2) \equiv \omega^2 = \mu_1(1 - \cos\varepsilon_1) + \mu_2(1 - \cos\varepsilon_2) + \omega_n^2, \tag{32}$$

where $\mu_1 = 2k_1/m$, $\mu_2 = 2k_2/m$ and $\omega_n^2 = k/m$. The function Ω can be used in conjunction with the analysis of the previous sections to yield the impulse response of the system via equations (16) and (21); in this regard it can be noted that for the present case $\rho(\mathbf{x}) = m$, $V = 1$ and $\mathbf{f}(\mathbf{x}) = 1$.

The function Ω is shown in Figure 4 for the particular case $\mu_1 = 1{\cdot}0$, $\mu_2 = 0{\cdot}57$ and $\omega_n^2 = 0{\cdot}25$. The group velocity $c_g = \sqrt{(c_{g1}^2 + c_{g2}^2)}$ for this case is shown in Figure 5, and the direction of the energy flow $\psi = \tan^{-1}(c_{g2}/c_{g1})$ is shown in Figure 6. In considering Figures 5 and 6, it should be noted that $c_{g1} = \partial\Omega/\partial\varepsilon_1$ and $c_{g2} = \partial\Omega/\partial\varepsilon_2$, so that the group velocity is normal to the Ω contours which are shown in Figure 4; furthermore, the magnitude of the group velocity is equal to the modulus of the gradient of the Ω surface [11]. The method of stationary phase is based on finding the stationary points which satisfy equations (13) and (14) for a specified time t and response location $\mathbf{n} = (n_1\, n_2)$. The specification of t and $\mathbf{n}$ is equivalent to specifying c_g and ψ, and it follows that the stationary points lie at the intersections of a specified c_g contour (see Figure 5(b)) with a specified ψ contour (see Figure 6(b)). The c_g and ψ contours are superimposed in Figure 7 to aid in the visualization of this procedure; as an example, there are four stationary points associated with $n_1 = 25$, $n_2 = 16$ and $t = 96$ s (corresponding to $c_g = 0{\cdot}309$ bays/s and $\psi = 32{\cdot}6^\circ$) and these are highlighted in the figure. Contours corresponding to $J = 0$ are also shown in Figure 7: according to the analysis presented in section 2.2 these contours are associated with the occurrence of caustics. It is clear from Figure 7 that any two c_g and ψ curves which meet on a $J = 0$ contour are tangential to one another at the meeting (stationary) point. In this case a change in c_g for fixed ψ (equivalent to a change in t for fixed $\mathbf{n}$) will lead to a change in the number of stationary points, since the two curves will either fail to meet (no stationary point) or they will cross twice (two stationary points). This supports the statement made in section 2.2.2 that two additional stationary points arise in traversing a caustic and, furthermore, it is clear that these two stationary points merge into a single stationary point (with $J = 0$) on the caustic. A description of the numerical method used here to locate the stationary points, together with other details regarding the practical implementation of the method of stationary phase, can be found in the Appendix.

The method of stationary phase is an approximate method of evaluating the double integral which appears in equation (11). As mentioned in section 2.1, this integral can also be evaluated numerically, and if the trapezoidal rule is employed then equation (11)

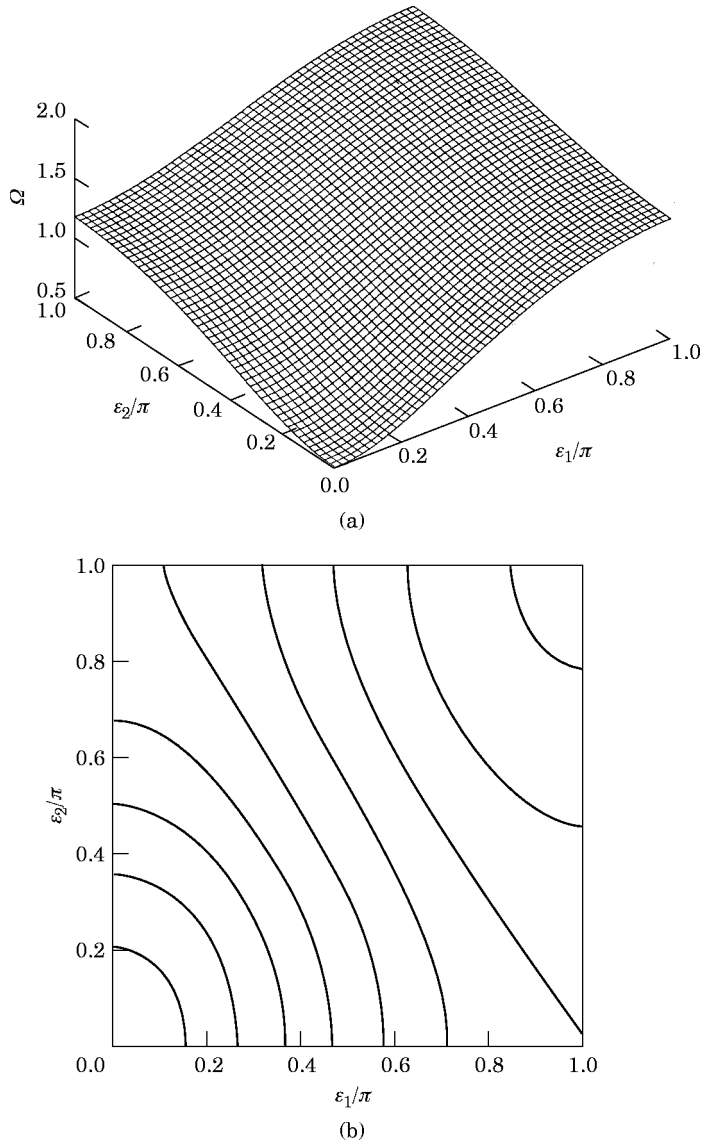

Figure 4. The phase constant surface $\Omega(\varepsilon_1, \varepsilon_2)$ for the example system: (a) surface plot; (b) contour plot with evenly spaced contours ranging from $\Omega = 0{\cdot}6$ to $\Omega = 1{\cdot}8$ in increments of $0{\cdot}15$.

reduces to equation (7). Now equation (7) is actually an exact result for the impulse response of a system of dimension $N_1 \times N_2$ which is subjected to Born–von Kármán (or periodic) boundary conditions; for times prior to the disturbance reaching the boundary this response is identical to that of an infinite system, and equation (7) may therefore be employed to assess the accuracy of the method of stationary phase. Given that the notion of periodic boundary conditions underlies all of the present analysis, and that this notion is somewhat artificial, it is useful to consider an independent analysis of the response of the system which can be used to validate the present approach. For this reason the impulse response of the example system has been computed by using direct numerical simulation, and an outline of the simulation procedure adopted is given in the following section.

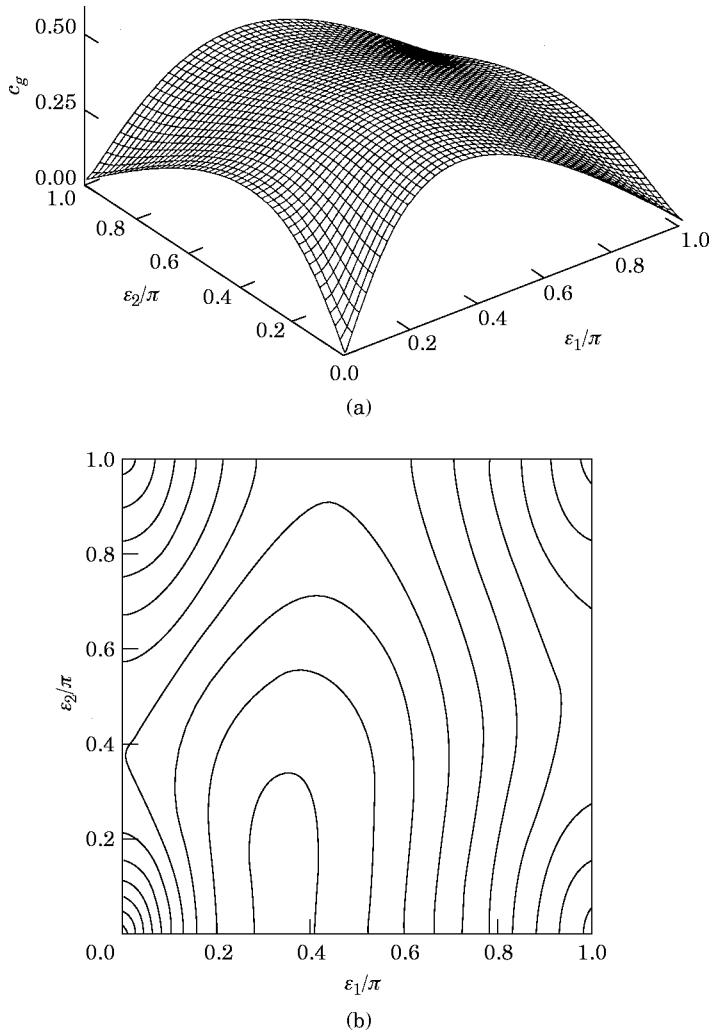

Figure 5. The group velocity $c_g(\varepsilon_1, \varepsilon_2)$ for the example system: (a) surface plot; (b) contour plot with evenly spaced contours ranging from $c_g = 0{\cdot}04$ to $c_g = 0{\cdot}49$ in increments of $0{\cdot}05$.

3.2. DIRECT NUMERICAL SIMULATION OF THE IMPULSE RESPONSE

For a finite system consisting of $N_1 \times N_2$ masses, the equations of motion represented by equation (30) can be expressed in the matrix form

$$\ddot{\mathbf{w}} = -(1/m)\mathbf{K}\mathbf{w}, \tag{33}$$

where the vector $\mathbf{w}$ contains the system displacements w_{ij} and the entries of the matrix $\mathbf{K}$ can readily be deduced from equation (30). For simplicity, the masses which lie on the edges of the system have been taken to be unrestrained here, so that the system has "free" boundary conditions. Equation (33) can be integrated numerically by any one of a variety of techniques; in the present work a simple difference scheme has been used so that

$$\mathbf{w}(t + \Delta t) = \mathbf{w}(t) + \dot{\mathbf{w}}(t)\Delta t, \qquad \dot{\mathbf{w}}(t + \Delta t) = \dot{\mathbf{w}}(t) - (\Delta t/m)\mathbf{K}\mathbf{w}(t), \tag{34, 35}$$

where Δt is the adopted time step. The initial conditions associated with an impulse of unit intensity applied to the ijth mass are $\mathbf{w}(0) = \dot{\mathbf{w}}(0) = \mathbf{0}$, apart from $\dot{w}_{ij}(0) = 1/m$. The

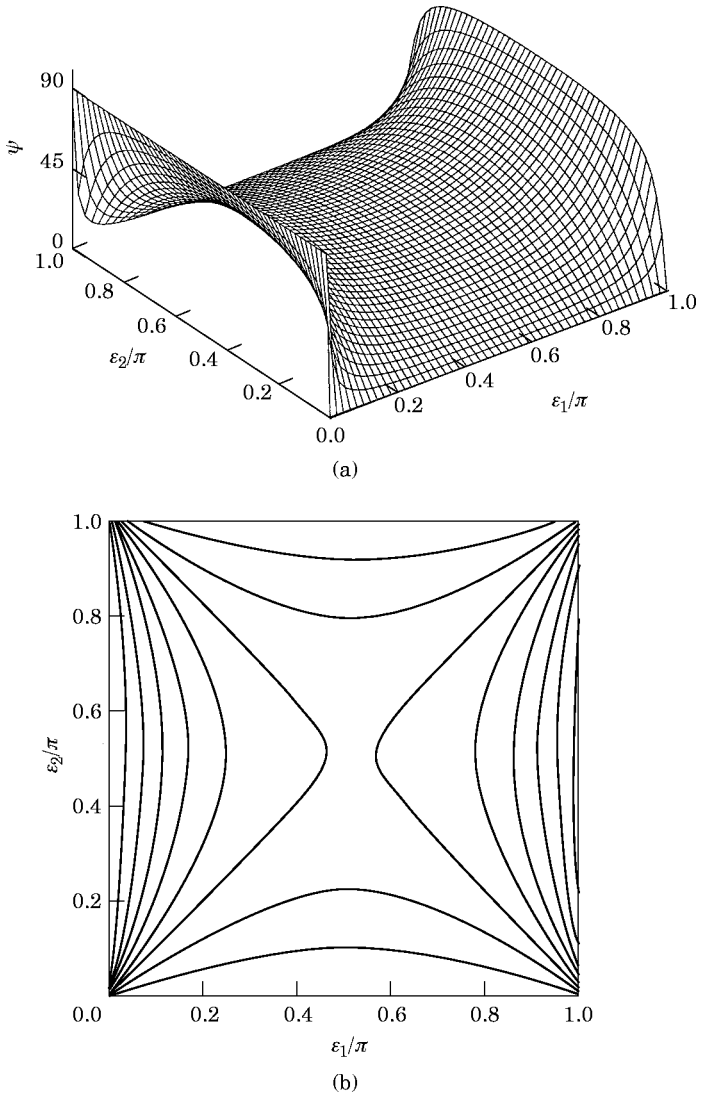

Figure 6. The direction of energy propagation $\psi(\varepsilon_1, \varepsilon_2)$ for the example system: (a) surface plot; (b) contour plot with evenly spaced contours ranging from $\psi = 10^\circ$ to $\psi = 80^\circ$ in increments of 10°.

application of equations (34) and (35) is computationally intensive in comparison to the methods presented in section 2, since the time step Δt must be small enough to guarantee the stability and accuracy of the scheme. Furthermore, the system size must be chosen to ensure that no reflections arise from the system boundaries over the time span that is considered.

3.3. RESULTS

The results that are presented in this section relate to the example system $\mu_1 = 1{\cdot}0$, $\mu_2 = 0{\cdot}57$ and $\omega_n^2 = 0{\cdot}25$, which was considered in section 3.1. Initially, the concept of using the modes of vibration associated with periodic boundary conditions has been validated by comparing the results yielded by equation (7) with numerical simulation results for the case $N_1 = N_2 = 20$ (with the reference system positioned so that $-10 \leqslant n_i \leqslant 9$ for $i = 1, 2$).

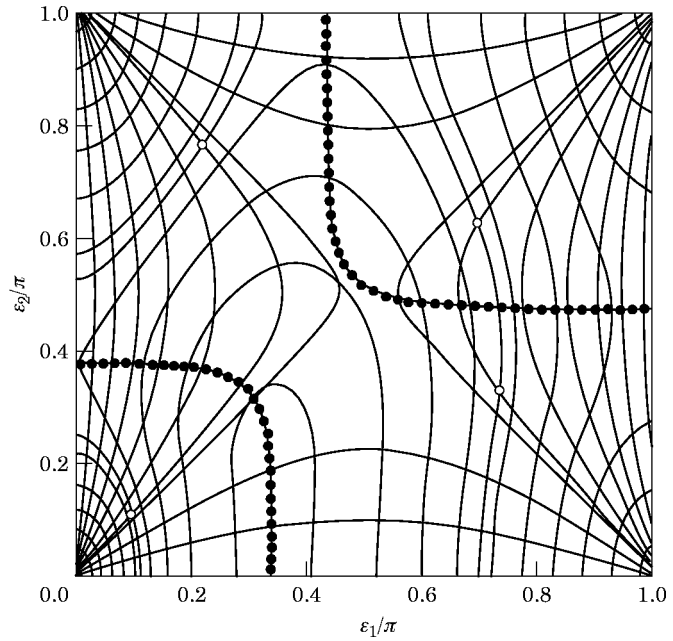

Figure 7. Superposition of the group velocity (c_g) and energy direction (ψ) contours for the example system. ○, The intersection of the contours $c_g = 0{\cdot}309$ and $\psi = 32{\cdot}6^\circ$; ●, those combinations of ε_1 and ε_2 for which $J = 0$.

The response at three points on the system produced by an impulse applied at $n_1 = n_2 = 0$ is shown in Figure 8 for times up to 15 s, which is prior to any reflection from the system boundaries. The results yielded by the two methods are virtually indistinguishable, and this confirms the validity of equation (7). It can be noted that the evaluation of equation (7) for every mass in the system takes a fraction of the computation time needed for the numerical simulation; furthermore, the numerical simulation requires the response of all

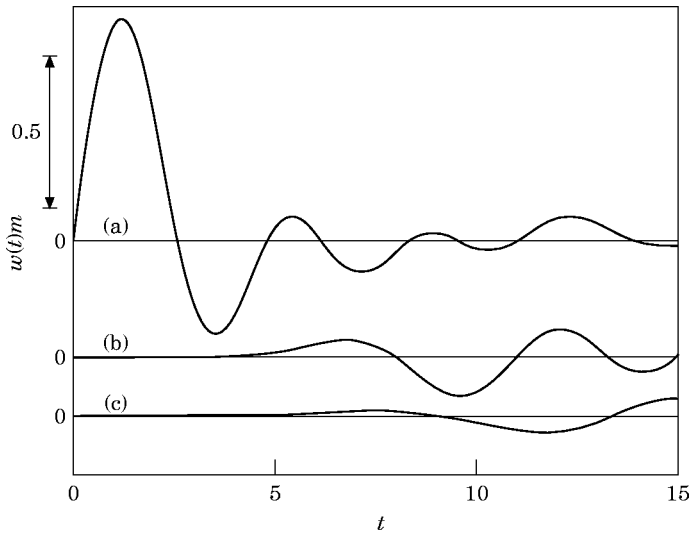

Figure 8. The response of the example system to an impulse of unit strength applied at the position $\mathbf{n} = (0\ 0)$: (a) the response at $\mathbf{n} = (0\ 0)$; (b) the response at $\mathbf{n} = (4\ 1)$; (c) the response at $\mathbf{n} = (4\ 1)$. In each case, two (nearly coincident) curves are shown, corresponding to numerical simulation and the use of equation (7).

the masses to be computed, whereas equation (7) can be applied independently to individual masses of particular interest. The anisotropy of the periodic system is clearly visible in the results which are shown in Figure 8, in the sense that the disturbance reaches the point (4, 1) before it reaches the point (1, 4). This is consistent with the fact that the group velocity of waves propagating in the n_1 direction generally exceeds that of waves propagating in the n_2 direction, as can be deduced from Figures 5 and 6.

A comparison between the results yielded by equation (7) and the method of stationary phase is shown in Figure 9, where in this case a system of dimension $N_1 = N_2 = 100$ has been considered in the evaluation of equation (7). The number of stationary points occurring in the method of stationary phase is indicated on the figure: for example at $\mathbf{n} = (4, 1)$ there are no stationary points for $t < 8{\cdot}3$, two stationary points for $8{\cdot}3 < t < 11{\cdot}93$, and four stationary points for $t > 11{\cdot}93$. The times $t = 8{\cdot}3$ and $t = 11{\cdot}93$ therefore represent caustics, and the analysis presented in sections 2.2.1 and 2.2.2 must be employed in the vicinity of these values of t. This procedure is illustrated in Figure 10, which concerns the effect of the caustic at $t = 11{\cdot}93$. If equation (16) is employed throughout the neighbourhood of the caustic, then a very large response is obtained at times immediately following the caustic (since $|J| \approx 0$ at the relevant stationary points), and a poor response estimate is obtained at times prior to the caustic (due to the neglect of the presence of the stationary point at the caustic). These effects are corrected by the application of equations (21), (22) and (28) prior to the caustic and equations (21), (22) and (23) following the caustic, as shown in Figure 10.

It can be seen from Figure 9 that the method of stationary phase generally yields a good estimate of the response of the system. The method becomes more accurate with increasing t and with increasing distance from the impulse location, which is consistent with the basic assumptions which lie behind the technique [10]. The method is largely analytic, and it

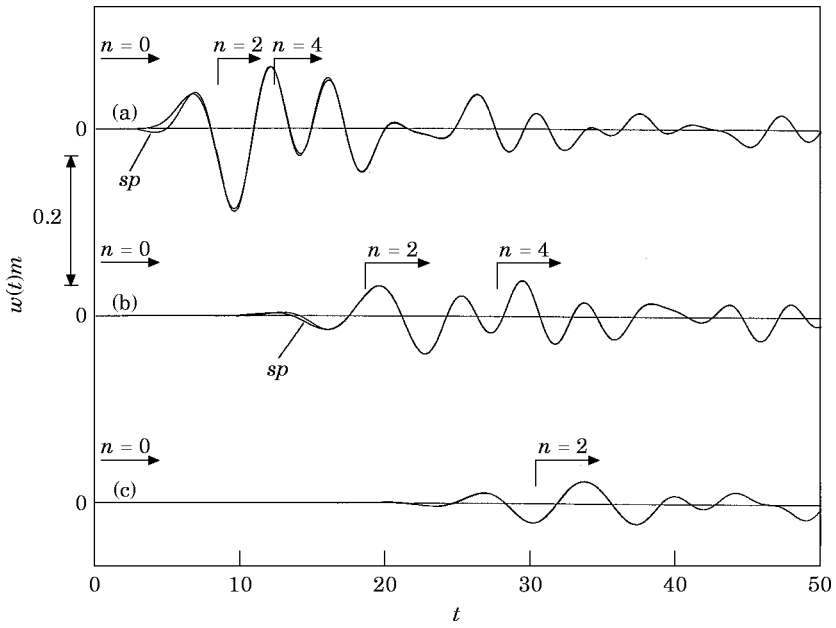

Figure 9. The response of the example system to an impulse of unit strength applied at the position $\mathbf{n} = (0, 0)$: (a) the response at $\mathbf{n} = (4, 1)$; (b) the response at $\mathbf{n} = (9, 1)$; (c) the response at $\mathbf{n} = (9, 9)$. In each case two curves are shown, corresponding to the use of equation (7) and the method of stationary phase (labelled *sp*). The values of n shown on the figure correspond to the number of stationary points arising in the method of stationary phase.

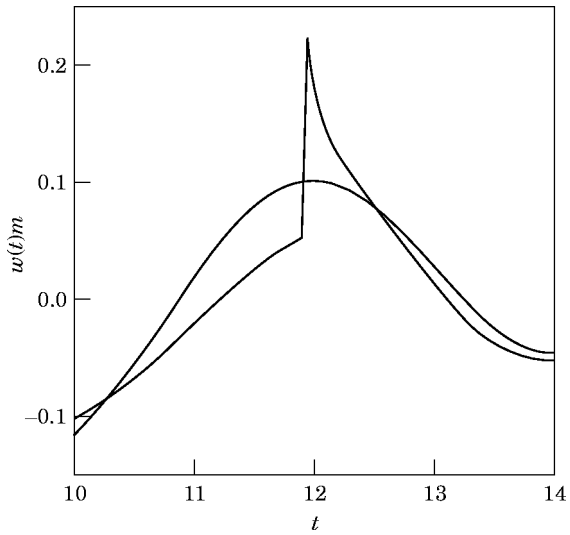

Figure 10. Details of the response at the point (4, 1) in the vicinity of the caustic occurring at $t = 11{\cdot}93$ s. The irregular curve is given by equation (16), while the smooth curve has been obtained by using the analysis detailed in sections 2.2.1 and 2.2.2.

therefore requires significantly less computation time than the direct numerical evaluation of equation (7)—the computational effort lies mainly in the determination of the stationary points. Although not reported in detail here, the method has been applied to other systems covering a range of values of μ_1, μ_2 and ω_n^2. With one exception, the method has been found to yield results which are of comparable accuracy to those shown in Figure 9; the exception concerns the case $\omega_n^2 = 0$, for which the function $\Omega(\varepsilon_1, \varepsilon_2)$ defined by equation (32) is not twice differentiable at the origin $\varepsilon_1 = \varepsilon_2 = 0$. In this particular case, the method of stationary phase is not applicable, although the method continues to perform well for values of ω_n^2 as low as 0·01. For $\omega_n^2 = 0$ resort must be made to equation (7).

The nature of the impulse response of the example system as a whole is shown in Figures 11–13, where the contours corresponding to $w = 0$ at a particular time are shown in each figure. The anisotropy of the system, which was mentioned in connection with Figure 9, is clearly evidenced in the non-circular shape of the disturbance wavefront. Much more revealing, however, are the results shown in Figure 14, which concern the spatial distribution of the maximum value of $|w|$ produced by the impulse—this figure has been constructed by computing the time history of w for each mass and thence finding the maximum value of $|w|$ achieved by each mass. These results can be compared with the spatial distribution of the response reported in reference [6] for the case of harmonic excitation: two distinct types of response were found to occur, depending upon the excitation frequency. In the first case, the magnitude of the response was found to vary smoothly with the polar angle $\psi = \tan^{-1}(n_2/n_1)$, and all parts of the structure exhibited a significant dynamic response. In the second case, the response varied in a complex way with the polar angle ψ, and a "dead zone" of almost zero response was obtained for a region centred on $\psi = 90^\circ$ (and also, symmetrically, at $\psi = -90^\circ$). This latter behaviour was traced to the existence of a critical angle of ψ at certain frequencies (referred to as the caustic direction ψ_c in reference [6]): at such frequencies all possible propagating waves transmit energy at a heading less than ψ_c to the n_1-axis, and thus the response at polar angles greater than ψ_c (in fact, $\psi_c \leqslant \psi \leqslant 180 - \psi_c$ and $-\psi_c \geqslant \psi \geqslant -180 + \psi_c$) is extremely low. Now, in accordance with the Fourier theorem, the impulse response which

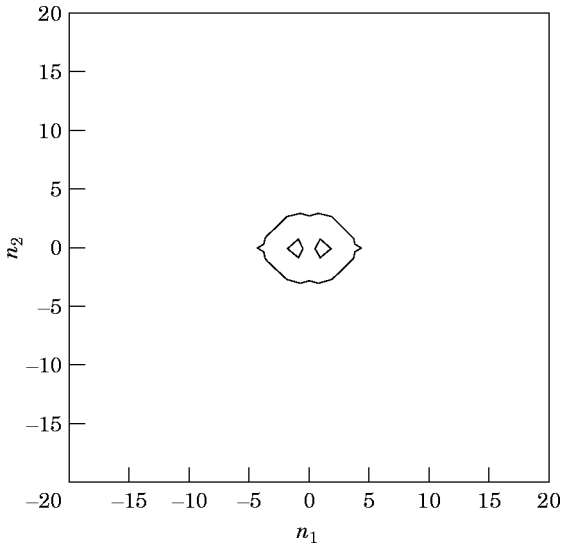

Figure 11. Contours of $w = 0$ at $t = 7{\cdot}5$ s.

is shown in Figure 14 contains contributions from all frequencies, and therefore the spatial distribution of $|w|$ can be expected lie somewhere between the two distinct forms of response reported in reference [6]. This is in fact the case, and the response shown in Figure 14 retains a distinctive spatial pattern. Clearly, $|w|$ has a strong dependency on ψ and, as mentioned in reference [6], this introduces the possibility of using the periodic structure as a spatial filter to isolate a sensitive item of equipment from an excitation source.

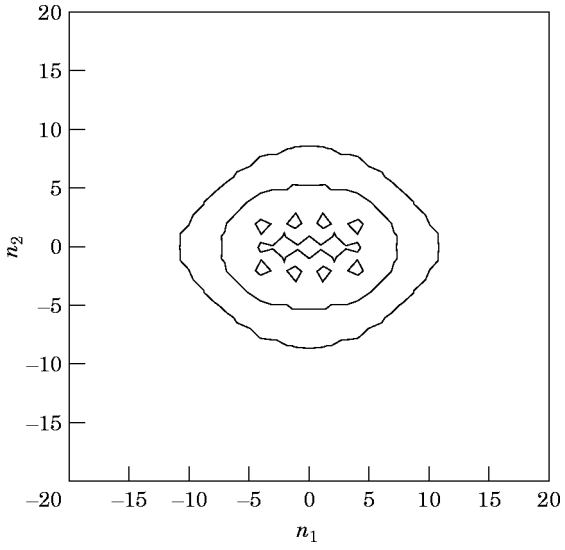

Figure 12. Contours of $w = 0$ at $t = 15$ s.

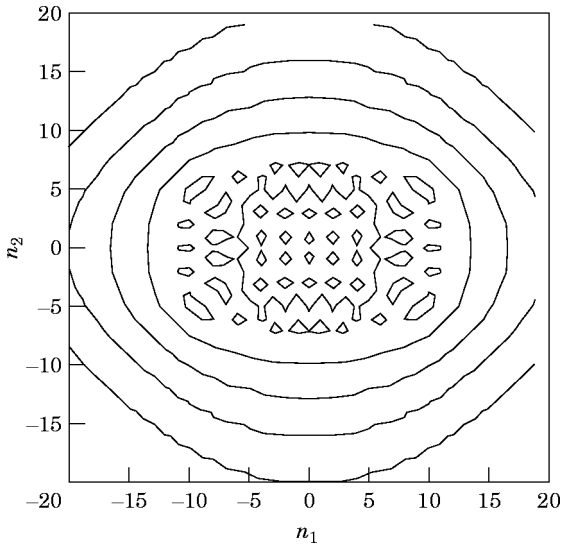

Figure 13. Contours of $w = 0$ at $t = 30$ s.

4. CONCLUSIONS

It has been shown that the response of a two-dimensional periodic structure to an impulsive point load can be computed efficiently by using the method of stationary phase. Equation (16) forms the key result of the method, although this equation must be replaced by equation (21) in the vicinity of a caustic. As discussed in section 2.2. the details of the functions G and A which appear in equation (21) depend upon whether the time of interest lies before or after the occurrence of the caustic: in the first case, equation (22) and (28) should be employed; whereas in the second case, equations (22) and (23) are appropriate. The information needed for the application of the method to an arbitrary two-dimensional periodic structure consists of the phase constant surface(s) $\Omega(\varepsilon_1, \varepsilon_2)$ and the associated

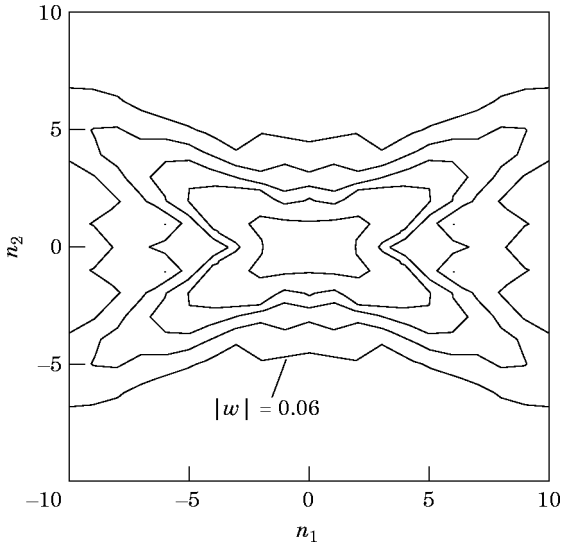

Figure 14. Contours of the maximum response $|w|$; the levels shown are 0·06, 0·08, 0·1, 0·12 and 0·2.

waveform(s) $\mathbf{f}(\mathbf{x})$, both of which are yielded by standard techniques for the analysis of free wave motion in periodic structures [2, 9]. It can be noted that the impulse response of a periodic system can also be computed by using equation (7); this approach is computationally more intensive than the method of stationary phase, although it avoids the need for higher order derivatives of the phase constant surface $\Omega(\varepsilon_1, \varepsilon_2)$—equation (7) might therefore offer advantages for a complex structure in which $\Omega(\varepsilon_1, \varepsilon_2)$ is found numerically rather than analytically.

The application of the method of stationary phase to a simple lumped mass system has shown that the spatial distribution of the maximum response $|w|$ can display a complex pattern which is closely related to the behaviour of the system under harmonic point loading [6]. As discussed in reference [6], this behaviour could possibly be exploited to reduce vibration transmission along a specified path, although the practicality of this approach for a complex system has yet to be investigated.

REFERENCES

1. S. S. Mester and H. Benaroya 1995 *Shock and Vibration* **2**, 69–95. Periodic and near-periodic structures.
2. D. J. Mead 1996 *Journal of Sound and Vibration* **190**, 495–524. Wave propagation in continuous periodic structures: research contributions from Southampton, 1964–1995.
3. D. J. Mead, D. C. Zhu and N. S. Bardell 1988 *Journal of Sound and Vibration* **127**, 19–48. Free vibration of an orthogonally stiffened flat plate.
4. N. S. Bardell and D. J. Mead 1989 *Journal of Sound and Vibration* **134**, 55–72. Free vibration of an orthogonally stiffened cylindrical shell, part II: discrete general stiffeners.
5. D. J. Mead 1990 *Journal of the Acoustical Society of America* **88**, 391–401. Plates with regular stiffening in acoustic media: vibration and radiation.
6. R. S. Langley 1996 *Journal of Sound and Vibration* **197,** 447–469. The response of two-dimensional periodic structures to point harmonic forcing.
7. L. Meirovitch 1986 *Elements of Vibration Analysis*. New York: McGraw-Hill; second edition.
8. L. Brillouin 1946 *Wave Propagation in Periodic Structures*. New York: Dover.
9. D. J. Mead 1973 *Journal of Sound and Vibration* **27**, 235–260. A general theory of harmonic wave propagation in linear periodic systems with multiple couplings.
10. M. J. Lighthill 1978 *Waves in Fluids*. Cambridge: Cambridge University Press.
11. R. S. Langley 1994 *Journal of Sound and Vibration* **172**, 491–511. On the modal density and energy flow characteristics of periodic structures.

APPENDIX: DETAILS OF THE ANALYTICAL METHOD

The method of stationary phase which is presented in section 2.2. is based on solving equations (13) and (14) to yield the stationary points in the ε_1–ε_2 plane for a specified response location $\mathbf{n} = (n_1\, n_2)$ and time t. As discussed in section 2.2. the specification of $\mathbf{n}$ and t is equivalent to specifying the group velocity of a periodic wave, since it follows from equations (13) and (14) that $c_{g1} = \partial\Omega/\partial\varepsilon_1 = n_1/t$ and $c_{g2} = \partial\Omega/\partial\varepsilon_2 = n_2/t$ (in the notation of section 3.1. $c_{g1} = c_g \cos\psi$ and $c_{g2} = c_g \sin\psi$). The phase constants ε_1 and ε_2 which are associated with specified values of c_{g1} and c_{g2} can be found by noting from equation (32) that

$$c_{g1} = \mu_1 \sin\varepsilon_1/2\Omega, \qquad c_{g2} = \mu_2 \sin\varepsilon_2/2\Omega. \tag{A1, A2}$$

The numerical solution of these two simultaneous non-linear algebraic equations in ε_1 and ε_2 yields the stationary points; in the present work the equations have been solved by first expressing ε_2 in the form $\varepsilon_2 = \sin^{-1}[(c_{g2}\mu_1/c_{g1}\mu_2) \sin\varepsilon_1]$, and then substituting this expression into equation (A1) to yield a non-linear equation in ε_1, which is solved by a search

technique (with due account taken of the fact that the expression for ε_2 yields two values over the range 0 to π). Having found the stationary points, equation (16) or equation (21) is then used to yield the system response: as explained in sections 2.2.1. and 2.2.2. equation (21) should be used in the vicinity of a caustic, which can be identified as a time at which the number of stationary points either increases or decreases. The partial derivatives of Ω which are needed for the evaluation of the terms G and A which appear in equation (21) are given by

$$\frac{\partial^{n+m}\Omega}{\partial^n p_1\,\partial^m p_2} = \left(\cos\theta\,\frac{\partial}{\partial\varepsilon_1} + \sin\theta\,\frac{\partial}{\partial\varepsilon_2}\right)^n \left(-\sin\theta\,\frac{\partial}{\partial\varepsilon_1} + \cos\theta\,\frac{\partial}{\partial\varepsilon_2}\right)^m \Omega, \tag{A3}$$

where θ is given by equation (19) and the partial derivatives of Ω with respect to ε_1 and ε_2 are readily found from equation (32).